Phonon-mediated drag at $\nu = 1/2$: A test of the Chern-Simons composite fermion theory

Martin C. Bønsager[1], Yong Baek Kim[2], and A. H. MacDonald[1]
[1] *Department of Physics, Indiana University, Bloomington, Indiana 47405*
[2] *Department of Physics, The Ohio State University, Columbus, Ohio 43210*
(February 6, 2008)

We report on a study of the phonon-mediated frictional drag between two-dimensional electron layers at the Landau level filling factor $\nu = 1/2$ predicted by Chern-Simons composite-fermion theory. Frictional drag between widely spaced layers is dominated by the phonon-mediated interaction and is altered from its zero-field form because of the large composite-fermion effective mass and, less strongly, by magnetic local-field effects. We find that the reduced drag resistance $\rho(T)/T^2$ peaks at a larger temperature and has a different density dependence than at zero field. We compare these results with recent experimental findings.

I. INTRODUCTION

Comparisons between measured transport properties and theoretical predictions have been fruitful in providing important information about elementary excitations in electronic systems. A recent and rather unusual example may be found in studies of the frictional drag between separately contacted, nearby, two-dimensional electron layers. Because it is a measure of the interlayer scattering rate, drag resistance is sensitive to Coulomb and phonon-mediated interactions between the layers and is related to correlated density fluctuations in the coupled bilayer system. Since these depend crucially on underlying electronic degrees of freedom, frictional drag can serve as an important test of specific theoretical predictions concerning the fluctuation spectrum of a given electronic system. At zero field, these studies have verified many qualitative features predicted by the random phase approximation (RPA) theory of correlations in moderate density two-dimensional electron systems. On the other hand, they have also demonstrated the importance, at a quantitative level, of various corrections. These studies have a greater potential importance in the fractional quantum Hall regime, where simple perturbative RPA-like theories fail and our understanding of correlations is much less complete. In the fractional quantum Hall regime, all electrons share the same quantized kinetic-energy and low-energy properties are entirely determined by electron-electron interactions. Electrons in the fractional quantum Hall regime are in the limit of extreme correlations. It is the failure of perturbation theory which admits all the peculiarities and surprises which have been discovered in this field over the past two decades.

One example of a peculiar strong-correlation consequence is presented by the Fermi-liquid-like properties of the compressible states which occur when the lowest Landau level is half-filled. Experimental evidence then supports the existence of gapless fermionic excitations which form a Fermi surface.[1] This is particularly surprising because the kinetic energy of the electrons in the lowest Landau level is quenched by the large magnetic fields, so this Fermi surface must result purely from interaction effects. On the theoretical front, the Chern-Simons composite fermion theory has been spectacularly successful in explaining various experimental findings at the phenomenological level[2,3]. It starts from a singular gauge transformation which attaches two flux quanta to each electron. These new 'composite particles', like electrons, obey Fermi statistics and are therefore called composite fermions. At $\nu = 1/2$, the mean-field flux-density from the attached flux quanta exactly cancels that coming from the external magnetic field. Neglecting fluctuations, composite fermions at $\nu = 1/2$ therefore experience zero magnetic field and have a Fermi surface. In the random phase approximation (RPA), the density-density correlation function for composite fermions is equal to the density-density correlation function for completely spin-polarized electrons at zero magnetic field. However, the density-density correlation function of the physical electrons contains an additional local field term associated with the attached flux quanta. We will refer to this additional term as the magnetic local field. In RPA theory, the magnetic-field dependence of the correlation function is completely embedded in this quantity.

Chern-Simons theory has the advantage of being technically and conceptually simple. It suffers, however, from various problems, most associated with the composite fermion mass scale m^*. On physical grounds, it is known that m^* is determined by the interaction energy scale in the lowest Landau level. However, the theory does not have a proper lowest Landau level projection so that m^* has to be fixed phenomenologically. Unfortunately, this naive approach leads to a violation of the f-sum rule and Kohn's theorem[4] in the sense that certain response functions should contain the bare electron mass m_b. A scheme to correct for this deficiency was developed by Simon and Halperin[5] who introduced the Modified Random Phase Approximation (MRPA). The MRPA includes a Fermi Liquid like correction, and allows for an effective mass m^* different from the band mass m_b while still satisfy-

ing the f-sum rule and Kohn's Theorem. Even though this prescription turns out to be surprisingly successful, a more microscopic understanding of the role of the lowest Landau level projection in the theory is desirable.

Recently several attempts have been made to construct a truly lowest Landau level theory of composite fermions.[6–12] Inspired by $\nu = 1/2$ variational wavefunction[6], it has been realized that the position of an electron and a nearby zero of the wavefunction (called a 'vortex') are displaced by $k_i l_B^2$ for each electron labeled by $i = 1, \cdots, N$. The lowest Landau level constraint and strong correlations tend to bind vortices to electrons. The composite object that consists of an electron and two vortices satisfies fermionic statistics and, as a result, the k_i's have to be chosen differently for each composite object. The ground state of these 'neutral composite fermions' is given by a Fermi sea in the space of k_i. One can also show that k_i acts as the guiding-center-translation generator in the lowest Landau level. Within a Hartree-Fock theory of these composite objects, the effective kinetic energy has the form $k_i^2/2m^*$ with an effective mass m^* given correctly by the interaction energy scale[6–12]. A self-consistent theory of neutral dipolar composite fermions has been constructed and it has been shown that, in the long-wavelength low-energy limit, this theory (taking the bare electron mass to infinity to reflect the absence of a kinetic energy term in the lowest Landau level Hamiltonian) gives the same physical response functions as those of the Chern-Simons composite fermion theory[10,11]. Coulomb mediated frictional drag between two $\nu = 1/2$ systems depends mostly on the long wavelength and low energy limits of density-density correlation in each layer. As a result, the two theories mentioned above should make identical predictions for Coulomb drag. This quantity has been measured[13] and the observations are consistent at relatively high temperatures with the theoretically predicted $T^{4/3}$ power law.[14–16] The data does, however, exhibit a low temperature anomaly that has not yet been fully understood.[17,18]

When two 2D electron systems are widely separated, the contribution to drag from Coulomb scattering between the layers is suppressed and phonon mediated interaction dominates. Unlike the Coulomb drag case, phonon mediated drag is sensitive to density-density correlations in each layer at relatively high frequencies and at wavevectors comparable to the inverse interparticle separation. Therefore studies of phonon mediated drag should provide useful information about excitations at finite frequencies and at large wavevectors, leading to a test of the underlying theory at many different energy and length scales, not just at the long wavelength and low energy limits. Since the equivalence between Chern-Simons theory and the neutral dipolar composite fermion theories has been established only in the long wavelength and low energy limits, studies of phonon drag may reveal important differences between these two theories. As the first step to investigate the validity of these theories, in this paper we report on a comparison between recent measurements of frictional drag[19] between widely separated two-dimensional electron layers at $\nu = 1/2$ and Chern-Simons composite fermion theory predictions. We find some qualitative differences between observations and trends predicted by theory and speculate on their implications for the theory of the half-filled Landau level.

In the following section we review the theory of frictional drag and discuss some of the features that are important in analyzing drag at $\nu = 1/2$. The theoretical framework we use to describe frictional drag is based on earlier $B = 0$ work involving two of us.[20] While there are some issues in the theoretical literature[21–23] on frictional drag which are not completely settled, these do not impact on the conclusions we draw here and we do not discuss them further. In Sec. III we present numerical results for drag, calculated from (M)RPA composite-fermion theory, and compare these with recent experimental results obtained by Zelakiewicz *et al.*[19]. Our conclusions are presented in Sec. IV.

II. FRICTIONAL DRAG

When two or more electronic systems are placed in close proximity, their transport properties are interdependent. In particular, currents in one subsystem can induce (or 'drag') currents in other subsystems. The first drag experiments[24] were on coupled two-dimensional and three-dimensional electron system. Drag between two-dimensional layers has been measured in electron-electron[25,26], electron-hole[27], and recently in hole-hole[28] systems. In this paper we consider frictional drag between two two-dimensional electron gases embedded in a GaAs-AlGaAs double quantum well system. The quantum wells widths L are ~ 200 Å and are separated by a center-to-center distance d which is large enough to ensure that interlayer tunneling can be neglected ($d \gtrsim 300$ Å). We imagine a current density J_1 being drawn in the first layer while the second layer is an open circuit. To counter balance the stochastic drag force between the layers, an electric field E_2 will build up in the second layer. The transresistivity, ρ_{21}, is defined as

$$\rho_{21} \equiv E_2/J_1, \tag{1}$$

ρ_{21} depends on the strength of interlayer interactions and on the phase space available for interlayer scattering events.

Theoretical expressions for ρ_{21} can be derived by conventional linear response theory at various levels of sophistication.[29–32] Under conditions which are met in current experiments, the transresistivity is given by

$$\rho_{21} = \frac{-\hbar^2}{8\pi^2 e^2 n_1 n_2 k_{\rm B} T} \int_0^\infty dq\; q^3 \int_0^\infty d\omega \left| \frac{W_{21}(q,\omega)}{\varepsilon(q,\omega)} \right|^2 \frac{{\rm Im}\Pi_1(q,\omega){\rm Im}\Pi_2(q,\omega)}{\sinh^2(\hbar\omega/2k_{\rm B}T)}. \tag{2}$$

Here n_i and $\Pi_i(q,\omega)$ are the two-dimensional electron density and the polarization function, respectively, of layer i. In Eq. (2) $W_{ij}(q,\omega)$ is the reciprocal space interaction between layers i and j, and $\varepsilon(q,\omega)$ is the interlayer screening function, given by

$$\varepsilon = [1+W_{11}\Pi_1][1+W_{22}\Pi_2] - W_{21}^2\Pi_1\Pi_2. \tag{3}$$

Given the interlayer interaction, this theory of frictional drag depends only on the polarization functions of the 2D electron layers.

Both interlayer Coulomb interactions and phonon-mediated interactions contribute to interlayer friction:

$$W_{ij}(q,\omega) = U_{ij}(q) + \mathcal{D}_{ij}(q,\omega). \tag{4}$$

Taking account of the finite quantum well widths, the Coulomb contribution is

$$U_{ij}(q) = \frac{e^2}{2\kappa q} B_{ij}(qd, qL/2) \tag{5}$$

where κ is the dielectric constant of the semiconductor and B_{ij} is a width-dependent form factor[20]. The phonon mediated interaction is given by

$$\mathcal{D}_{ij}(q,\omega) = \sum_\lambda \int \frac{dQ_z}{2\pi\hbar} |M_\lambda(\mathbf{Q})|^2 F_i(Q_z) F_j(-Q_z) D_\lambda(\mathbf{Q},\omega) \tag{6}$$

where $F_i(Q_z) = \int dz |\varphi_i(z)|^2 e^{-iQ_z z}$ is the Fourier transform of the electron density in the direction perpendicular to the layers (φ_i is the subband wavefunction in layer i), and $D_\lambda(\mathbf{Q},\omega)$ is the phonon propagator. We use the notation $\mathbf{Q} = (\mathbf{q}, Q_z)$. The index λ denotes longitudinal and transverse phonon modes, $\lambda = l, t$. Both acoustic and optical phonons can contribute to drag, but in GaAs/AlGaAs systems acoustic phonons dominate under the conditions studied in this paper.[33,34] The electron-acoustic phonon coupling matrix elements are given by[35,36]

$$|M_l(\mathbf{Q})|^2 = \frac{\hbar Q}{2\varrho c_l}\left[D^2 + (eh_{14})^2 \frac{9q^4Q_z^2}{2Q^8}\right] \tag{7}$$

$$|M_t(\mathbf{Q})|^2 = \frac{\hbar}{2\varrho c_t}(eh_{14})^2 \frac{8q^2Q_z^4 + q^6}{4Q^7} \tag{8}$$

where the c_λ are the phonon velocities for longitudinal and transverse phonons, ϱ is the mass density of GaAs/AlGaAs, D is the deformation potential, and eh_{14} is the piezoelectric constant. In our numerical evaluations we use $c_l = 5140$ m/s, $c_t = 3040$ m/s, $\varrho = 5300$ kg/m^3, $D = -13.0$ eV, and $eh_{14} = 1.2\times10^9$ eV/m.

Because their contributions come dominantly from different regions of wavevector and frequency, it is possible, both experimentally and theoretically, to separate Coulomb and phonon-mediated contributions to drag. Coulomb drag comes from $q \lesssim d^{-1}$, whereas phonon-mediated drag is dominated by contributions from $q \simeq 2k_F$ and frequencies at the peak in $\mathcal{D}_{ij}$ near $\omega = c_\lambda q$. Work at zero magnetic field has established that Coulomb drag dominates at small interlayer separations($d \sim 300$ Å) but falls off rapidly with increasing d. Phonon mediated drag, on the other hand, depends only weakly on d and has been observed for layers separated by distances approaching 1μm.

A. Frictional drag at $B = 0$

Frictional drag in the absence of a field is now well understood and the extensive literature has recently been reviewed.[37] Eq. (2), combined with the Random Phase Approximation for the 2D electron system polarization function, successfully[25] predicts a low-temperature drag $\rho_{21} \propto T^2$, a substantial enhancement[38–40] of ρ_{21} due to the excitation of plasmon modes at around half the Fermi temperature, and a crossover from Coulomb drag to phonon-mediated drag for layers separated by more than ~ 50nm. Phonon-mediated drag is readily identified by its signature dependences on the ratio of electron densities in the two layers and on temperature. For phonon-mediated drag $\rho_{21} \propto T^6$ at low temperatures ($T \sim 0.1$ K) and varies approximately linearly at higher temperatures ($T \gtrsim 5$ K). As a consequence the scaled transresistivity ρ_{21}/T^2, which is more nearly constant in the Coulomb case, will have a well defined peak. The origin of this peak in ρ_{21}/T^2 is easily understood by looking at Fig. 1 which shows the phonon resonance and the particle-hole continuum in phase space. The integrand in Eq. (2) is cut off exponentially with ω at $\hbar\omega \sim k_{\rm B}T$. The full phonon resonance is thus exploited when $T = T_{\rm peak} \sim \hbar c_\lambda 2k_F/k_{\rm B}$, and a further increase in the temperature will only lead to a relatively smaller increase in ρ_{21}.

The occurrence of a peak depends only on the phonon resonance and the existence of a Fermi surface, which leads to a sharp edge of the particle-hole continuum as shown in Fig. 1. The precise location of the peak, however, will depend on detailed properties of the polarization function at large q as well as on many other parameters of the experiment. At $B = 0$, good agreement with experiment for the overall shape of scaled transresistivity curves and for the location of their peaks corroborates the theory. Disagreements in magnitude can in part be attributed to uncertainties in the electron-phonon interaction parameters (ρ_{21} varies approximately as the fourth power of the deformation potential constant D and this parameter is not accurately known). Corrections to the RPA polarization function at large wavevector[20] may also play a role. Moreover, the magnitude of ρ_{21} depends on the phonon mean free path $\ell_{\rm ph}$ which appears in the phonon propagator. In Ref. 20 it was shown that for $\ell_{\rm ph}$ larger than a critical value $\ell_{\rm crit}$, the transresistivity is enhanced by to a collective mode (i.e. a zero in the real

part of the screening function near $q = 2k_F$). At zero magnetic field $\ell_{\rm crit} \sim 200$ μm for $n = 1.5 \times 10^{15}$ m^{-2}.

The view taken in this paper is that frictional drag is sufficiently well understood that it can be used to probe, at least at a qualitative level, the wavevector and frequency dependent polarization functions of the coupled 2D electron layers. Just such a probe is urgently needed to test composite fermion theory of the half-filled Landau level.

B. Coulomb drag at $\nu = 1/2$

Sakhi,[15], Ussishkin and Stern,[14] and Kim and Millis[16], using Chern-Simons RPA theory, independently predicted that at $\nu = 1/2$ the low-temperature transresistivity ρ_{21} would be greatly enhanced compared to its $B = 0$ value. In these theories $\rho_{21} \propto (T/d)^{4/3}$ for $T \to 0$. This property follows from the form of the Chern-Simons RPA polarization function in the limits $q \ll k_F$ and $\omega \ll v_F q$ (see Appendix A). Subsequent experiments by Lilly *et al.*,[13] did demonstrate increased drag which vanished less rapidly than T^2 with declining temperature. The experimental results are consistent with a $T^{4/3}$ law, except below ~ 0.5 K where the temperature dependence slows further and the drag value becomes sample specific.

In Chern-Simons RPA theory, the Coulomb drag enhancement is due to the diffusive character of composite-fermion density fluctuations at long wavelength and low frequency. In Fig. 2 we plot the Coulomb contribution to ρ_{21} (evaluated by numerical integration of Eq. (2)) as a function of d for different temperatures. The plot shows that for $T \gtrsim 0.1$ K, the transresistivity falls of approximately as d^{-2}, significantly slower than the d^{-4} behavior at $B = 0$, but still fast enough to guarantee that phonon-mediated drag will dominate for widely separated layers. The plots in Fig. 2 were calculated using the Chern-Simons RPA with an effective mass $m^* = m_{\rm e}$. In Fig. 3 we illustrate the dependence of Coulomb drag on the choice of the effective mass, and the difference between RPA and MRPA predictions. Phonon mediated drag which is dominated by short wavelengths is not enhanced by the diffusion-like pole in the polarization function.[41] It will, however, as we discuss below, be enhanced over the corresponding zero-field result. A numerical comparison shows that, generally, phonon-mediated drag will dominate over Coulomb drag for $d \gtrsim 200$ nm.

III. PHONON MEDIATED DRAG AT $\nu = 1/2$

Two qualitative aspects of the comparison between phonon-mediated drag at $\nu = 1/2$ and at $B = 0$ can be anticipated in advance of any detailed calculation. Firstly, since the polarization function is proportional to the effective mass, one would expect the phonon-mediated transresistivity to be larger at $\nu = 1/2$ by a factor of approximately $(m^*/m_b)^2 \sim 100$. Notice that this enhancement is weaker than for Coulomb drag which is enhanced by a factor of approximately 1000 (independent of mass for $T \to 0$). Secondly, the value of $T_{\rm peak}$ should be larger than at $B = 0$ for several reasons. The Fermi wavevector is increased by a factor of $\sqrt{2}$ if, as we assume here, the electron system is completely spin polarized. The smaller Fermi energy and Fermi velocity, which go along with the larger effective mass, should also increase $T_{\rm peak}$. For larger m^*, the ratio of the phonon velocity to the Fermi velocity approaches unity, and the most important drag contributions will then come from energies near the Fermi energy. Correspondingly, within the particle-hole continuum, the largest possible momentum transfer (which is given by $q = 2k_F(1 + c_\lambda/v_F)$) is larger at $\nu = 1/2$ than for $B = 0$ ($c_\lambda \ll v_F$ for $B = 0$). Furthermore, since $T_{\rm peak}$ is close to the Fermi temperature T_F, it is necessary to evaluate the polarization functions at finite temperature. (At finite T the Fermi gas polarization function can no longer be evaluated analytically. See Appendix A for a detailed discussion of its numerical evaluation.) When evaluated at finite temperature, the polarization function has finite contributions from outside the $T = 0$ particle-hole continuum (see Fig. 1). This additional effect suggests that a *further* increase of $T_{\rm peak}(\nu = 1/2)/T_{\rm peak}(B = 0)$ which should therefore be larger than $\sqrt{2}(1 + c_\lambda/v_F)$. Indeed our numerical calculations confirm this expectation which is not, however, in agreement with experiment.

Zelakiewicz *et al.*[19] have measured the transresistivity in samples with $d = 2600$ Å and $d = 5200$ Å where they find no evidence of a contribution from the Coulomb interaction. The transresistivity was indeed found to have the same qualitative features as at $B = 0$, except that the transresistivity is enhanced by a factor of ~ 200. The scaled transresistivity ρ_{21}/T^2 does have a peak as a function of temperature whose location scales with electron density as $\sqrt{n}$, just as in the $B = 0$ case. However, the value of $T_{\rm peak}$ was found to be slightly smaller at $\nu = 1/2$ than at $B = 0$. The detailed calculations we present below thus tend to indicate that Chern-Simons composite fermion theory overestimates electron polarizability at wavevectors $\sim 2k_F$, as anticipated by the authors of Ref. 19. Our calculations are similar to ones performed earlier[20] at $B = 0$; the most troublesome complication is the requirement that the free-particle polarization function be evaluated at finite temperatures. This aspect of the calculation is explained in detail in Appendix A.

Figs. 4, 5, and 6 show numerical evaluations of ρ_{21}/T^2 as a function of T for $m^* = 0.067m_e$, $m^* = 0.4m_e$ and $m^* = m_e$ respectively. Calculations at intermediate values of m^* interpolate smoothly between the trends illustrated in these three figures. The striking differences we find in the temperature and density dependences for the different values of m^* are due primarily to the different values of the Fermi temperature compared to the energy of an acoustic phonon with a wavelength comparable to

the distance between electrons. We concentrate first on the property which is most prominent in the experimental data, as conventionally presented, $T_{\rm peak}$. We discuss its dependence on density and the phenomenological mass parameter m^*. At zero magnetic field $T_{\rm peak} = 2.6$ K in a calculation which uses the same parameters as in Fig. 4. Fig. 4 shows results obtained when the band mass is used for m^* so that differences from the $B = 0$ case are due only to spin-polarization and the introduction of the magnetic local field. The local field increases the relative importance of small angle scattering and decreases $T_{\rm peak}$ below the naively expected value $\sqrt{2} \times 2.6$ K. This tendency of the local field is closely connected to the modification which changes the temperature dependence from T^2 to $T^{4/3}$ in the Coulomb drag case. Even with this effect, however, $T_{\rm peak}$ is safely above its zero field value, in disagreement with the experimental findings of Ref. 19. For this mass, $T_{\rm peak}$ increases with density approximately as $\sqrt{n}$ as in the $B = 0$ case.[20] The origin of this behavior is simply that the highest momentum transfer within the particle-hole continuum is proportional to $\sqrt{n}$ and that the Fermi temperature for these values of m^* is sufficiently high compared to $T_{\rm peak}$ that ${\rm Im}\Pi(q,\omega)$ has negligible weight outside the particle-hole continuum.

In Figs. 5 and 6 we see that $T_{\rm peak}$ is still larger at the larger values of m^* required to fit other data in the quantum Hall regime. This is in accord with the considerations outlined above. With increasing m^* the Fermi temperature decreases and momentum transfers greater than $2k_F$ receive more weight. For higher values of the mass, it is interesting to see that the value of $T_{\rm peak}$ has a more complex density dependence, reflecting a competition between two effects. As the density increases, the maximum possible momentum transfer increases, which tends to increase $T_{\rm peak}$. At the same time, however, the Fermi temperature increases which leads to a smaller contribution from outside the particle-hole continuum. This tends to decrease $T_{\rm peak}$. Because of this competition, the density-dependence of $T_{\rm peak}(n)$ changes from increasing at $m^* = 0.067m_e$, to decreasing at $m^* = 0.4m_e$, to approximately constant for $m^* > 0.4m_e$. As for the magnitude of the transresistivity, we see that for a phonon mean free path $\ell_{\rm ph} = 100$ μm, we would have to choose an effective mass in the neighborhood of $m^* = 0.3m_{\rm e}$ in order to match the experimental result that $\rho_{21}/T^2_{\rm peak} \simeq 200$ mΩ/K^2. (For this choice of parameters , the numerical results need to be multiplied by a factor of 5.7 to match the experimental results at zero magnetic field[42]).

Phonon mediated drag might not, however, be a good way of determining the effective mass of Composite Fermions. The critical phonon mean free path $\ell_{\rm crit}$ itself depends on m^* ($\ell_{\rm crit} \propto 1/(m^*)^2$) and will thus be different for $B = 0$ and $\nu = 1/2$. In Fig. 7 we plot the transresistivity as a function of $\ell_{\rm ph}$ for different values of m^*. At $\ell_{\rm ph} \simeq \ell_{\rm crit}$ a long-lived collective mode develops, leading to an enhancement of ρ_{21} before it saturates at $\ell_{\rm ph} \gg \ell_{\rm crit}$. The qualitative distance dependence is rather similar to the zero magnetic field case (see Ref. 20): For $\ell_{\rm ph} \ll \ell_{\rm crit}$, the transresistivity depends logarithmically on $d/\ell_{\rm ph}$, i.e. $\rho_{21} \propto \ln(Ad/\ell_{\rm ph})$ for $d \ll \ell_{\rm ph}/A$ where A is a constant of order $2k_FL$. For $d \gg \ell_{\rm ph}/A$ the transresistivity falls off exponentially, $\rho_{21} \propto \exp(-Ad/\ell_{\rm ph})/d$. If, on the other hand, the phonon mean free path is larger than the critical value $\ell_{\rm crit}$, the distance dependence is more complicated.

IV. DISCUSSION

In this paper we describe the dependence of phonon mediated drag at $\nu = 1/2$ on system parameters and composite fermion mass predicted by the Chern-Simons MRPA theory. We have focused on the characteristic temperatures $T_{\rm peak}$ at which the scaled drag resistivity $\rho_{21}(T)/T^2$ reaches its peak. Crudely we expect $k_BT_{\rm peak}$ to equal the phonon energy at the largest wavevector for which the two-dimensional electron systems have substantial charge fluctuations. Because of the sharp particle-hole continuum of Chern-Simons composite fermion theory, the maximum momentum transfer is close to $2k_F^{\rm cf}$, where $k_F^{\rm cf}$ is the Fermi wavevector of the composite fermion Fermi sea. These considerations lead to $T_{\rm peak} \sim \hbar c_\lambda 2k_F^{\rm cf}/k_B$. Since $k_F^{cf} = \sqrt{2}k_F$ for completely spin polarized composite fermions, $T_{\rm peak}$ at $\nu = 1/2$ should be larger than $T_{\rm peak}$ at $B = 0$, in disagreement with experiment. Our detailed calculations confirm that, at a qualitative level, this is indeed the prediction of Chern-Simons composite fermion theory.

At a quantitative level, the change of Fermi radius is not the only difference which arises in comparing phonon-mediated drag at $B = 0$ and at $\nu = 1/2$. One source of complication is the strong dependence of the drag resistivity on the effective mass m^* of the composite fermions. The large effective mass of composite fermions leads to a substantially smaller Fermi energy and Fermi velocity. This in turn leads to larger maximum momentum transfer, $q = 2k_F^{\rm cf}(1 + c_\lambda/v_F)$, since c_λ is then comparable to v_F. In addition, contributions to drag from outside the $T = 0$ particle-hole continuum increase. On the other hand, the magnetic local field correction increases the relative importance of small angle scattering and tends to decrease $T_{\rm peak}$. Because of these mutually competing effects, the position of the maximum is sometimes larger than value expected on the basis of naive considerations and quoted above. For example, when m^* is comparable to m_b, the Fermi temperature effect is relatively small and the magnetic local field effect leads to a $T_{\rm peak}$ smaller than the naive value. Nevertheless, the position of $T_{\rm peak}$ at $\nu = 1/2$ is *always* well above that of $B = 0$ case.

We now present a detailed summary of the comparison between our theoretical results and experiment[19]. The following aspects of the experimental data[19] are consistent with theoretical results.

1. The magnitude of the phonon mediated drag at $\nu = 1/2$ is about 200 times larger than at $B = 0$. In the theory, the factor of a few hundred comes from the enhanced density of states, $m^*/2\pi\hbar^2$, of composite fermions compared to the bare density of states, $m_b/2\pi\hbar^2$, of electrons at $B = 0$. $m^*/m_b \sim 10$ according to numerical and theoretical estimations[2]. The presence of two layers leads to $(m^*/m_b)^2 \sim 100$ fold enhancement in the drag rate.

2. When the phonon mean free path of $\ell_{ph} = 100\ \mu m$ is chosen consistently for $B = 0$ and $\nu = 1/2$, the experimental data can be fit by choosing m^* around $0.3m_e$ which is consistent with previous numerical and theoretical estimations[2].

3. There is a well defined maximum of ρ_{21}/T^2, suggesting that $\nu = 1/2$ systems have a fairly sharp wavevector cutoff for low-energy charge fluctuation, as predicted by Chern-Simons composite fermion theory.

On the other hand, the following experimental results do not agree with theoretical predictions.

1. Experimentally, $T_{\rm peak}$ at $\nu = 1/2$ is always smaller than that of $B = 0$. Theoretically it is always larger, even when unrealistically small values are used for the composite fermion effective mass.

2. Experimentally, $T_{\rm peak}$ is proportional to $\sqrt{n}$. Theoretically, this simple behavior is found only when unrealistically small values are used for the composite fermion effective mass.

We now discuss some possible sources of these discrepancies.

Incomplete spin polarization: In our calculations, we assumed complete spin polarization. If the spins are only partially polarized, the Fermi sea of the majority spin would be smaller than in the fully polarized case, leading to a smaller maximum momentum transfer and a smaller $T_{\rm peak}$. Recently the spin polarization of $\nu = 1/2$ state was measured by NMR[43,44]. In the experiment by S. Melinte et al.[43], the electron density, $n = 1.4\times10^{11}cm^{-2}$, of their sample M242 is similar to the density, $n = 1.5\times10^{11}cm^{-2}$, of the sample studied in the drag experiment of S. Zelakiewicz et al.[19]. In the NMR experiment[43], $\nu = 1/2$ is reached when the external magnetic field is $B = 11.4$ T, compared to the field strength $B = 12.82$ T for $\nu = 1/2$ in the drag experiment[19]. This NMR experiment can therefore be used to get a reasonable estimate of the $\nu = 1/2$ spin polarization in the drag experiment. We conclude that the spin polarization in the $\nu = 1/2$ drag experiment at $1-2$ K was about 70% of the full polarization. This would imply that majority-spin Fermi wavevector was $\sqrt{1.7}k_F \approx 1.3k_F$ and that of the minority spin Fermi wavevector is $\sqrt{0.3}k_F \approx 0.55k_F$. This reduction in the majority spin-wavevector ($1.3k_F$ compared to $\sqrt{2}k_F$) is not sufficient to explain the low $T_{\rm peak}$ values seen in the experiments. In our theory, we would not expect a large contribution to drag from the minority spins, and in any event the Fermi radius $0.55k_F$ is too small for it to be associated with the observed value of $T_{\rm peak}$ slightly below that of $B = 0$ case. We conclude that incomplete spin polarization alone cannot explain the discrepancy between theory and experiment.

Breakdown of (M)RPA at large wavevectors: This experimental result may signal that the (M)RPA is not adequate to describe the large wavevector response of a $\nu = 1/2$ system. It is generally accepted that Ward identities[45] related to conservation laws, limit beyond (M)RPA contributions to density-density and current-current response functions in the long wavevectors and low energy limit. However, it has been also shown that response functions at large wavevectors, in particular near $2k_F$, may be modified at low energies by singular vertex corrections[46]. Even though these singular corrections appear at low energies at $2k_F$, it is certainly possible that these singular corrections persist to higher energy scales comparable to $T_{\rm peak}$ or $\hbar c_\lambda 2k_F^{\rm cf}/k_B$. If this is true, it may be necessary to get beyond the (M)RPA to obtain an accurate description of phonon-mediated drag.

Dipolar Composite Fermions: As discussed in the introduction, there exist at present two descriptions of $\nu = 1/2$ composite fermions. It has been established that these two descriptions are equivalent in the low energy and long wavelength limits. However, these two descriptions may lead to quite different predictions at large wavevectors because dipolar composite fermions have a finite size which can be comparable to k_F^{-1}. Indeed, it has been observed that the equivalence of two approaches may break down at higher energies even in the long wavelength limit[12]. The singular behavior of the response functions near $2k_F$ mentioned above in the Chern-Simons theory approach may be a signature of the breakdown of the theory at large wavevector scales and a proper description of the system at large wavevectors may require the fully lowest Landau level dipolar composite-fermion theory. Calculations of the relevant response functions and of the drag resistivity in the dipolar composite fermion approach are in progress[47].

In conclusion, the Chern-Simons theory of composite fermions overestimates charge fluctuations at the Fermi wavelength scale and a proper description of the system at large wavevectors may have to take into account the extended nature of dipolar composite fermions.

V. ACKNOWLEDGEMENTS

This work was initiated at the Institute for Theoretical Physics in University of California at Santa Barbara (NFS grant PHY9407194), and was further supported by the NSF under grants DMR-9714055 (M.C.B

and A.H.M) and DMR-9983783 (Y.B.K.), by the Danish Research Academy (M.C.B), and by the A. P. Sloan Foundation (Y.B.K.). The authors are grateful T. J. Gramila, B. Y.-K. Hu, and S. Zelakiewicz, for informative and stimulating interactions. Y.B.K. would like to thank also Isaac Newton Institute at the University of Cambridge for the hospitality.

APPENDIX A: POLARIZATION FUNCTIONS

In this appendix we summarize the techniques we use to evaluate the free-fermion polarization functions which appear in Eq. (2) at finite temperatures and, for completeness, present explicit expressions for the (Modified) Random Phase Approximation polarization functions.

The electron polarization function $\Pi^{\rm e}(q,\omega)$ expresses the linear response of an electron system to the total electromagnetic field. For a two-dimensional system (in the x-y plane) and a magnetic induction restricted to the z-direction, $\mathbf{B} = B\hat{z}$, it is sufficient to consider the number density n and the y-component of the number current density j_y (j_x is fixed by particle conservation). In a 2-vector notation, the polarization function is defined by

$$j^\alpha(q,\omega) = ec^2\Pi^{{\rm e},\alpha\beta}(q,\omega)A^\beta_{\rm total}(q,\omega), \tag{A1}$$

where $\mathbf{j} = (cn, j_y)$ and $\mathbf{A} = (\Phi/c, A_y)$. The scalar potential Φ and vector potential $\mathbf{A}$ are related to the electric field $\mathbf{E}$ and the magnetic induction $\mathbf{B}$ is given by $\mathbf{E} = -\nabla\Phi$ and $\mathbf{B} = \nabla\times\mathbf{A}$ with $\nabla\cdot\mathbf{A} = 0$. This choice is known as the Coulomb gauge. The total field is the sum of the external field and the field induced by the current and charge response of the system.

The tensor $\Pi^{\rm e}(q,\omega)$ has four components $\Pi^{\rm e}_{00}$, $\Pi^{\rm e}_{01}$, $\Pi^{\rm e}_{10}$, and $\Pi^{\rm e}_{11}$, which are related by linear response theory to density-density, density-current, current-density, and current-current correlation functions, respectively. For the drag calculations we are only interested in the density-density response $\Pi^{\rm e}_{00}$ which is called $\Pi(q,\omega)$ in the main text.

$\Pi^{\rm e}(q,\omega)$ is known only approximately, even at $B = 0$. In the Random Phase Approximation, the polarization function correlation functions are approximated by their non-interacting fermion forms. At $B = 0$ we thus use $\Pi^{\rm e} = 2\Pi^{(0)}_{00}$ with

$$\Pi^{(0)}_{00} = \frac{1}{A}\sum_{\mathbf{k}}\frac{n_F(\xi_{\mathbf{k}+\mathbf{q}}) - n_F(\xi_{\mathbf{k}})}{\hbar\omega - \xi_{\mathbf{k}+\mathbf{q}} + \xi_{\mathbf{k}} + i\eta}. \tag{A2}$$

At zero temperature the wavevector integral can be evaluated analytically:[48]

$$\begin{aligned}{\rm Re}\Pi^{(0)}_{00} = \frac{g_0}{2z}\Big(&2z - C_-[(z-u)^2-1]^{1/2} \\ &-C_+[(z+u)^2-1]^{1/2}\Big)\end{aligned} \tag{A3}$$

$$\begin{aligned}{\rm Im}\Pi^{(0)}_{00} = \frac{g_0}{2z}\Big(&D_-[1-(z-u)^2]^{1/2} \\ &-D_+[1-(z+u)^2]^{1/2}\Big)\end{aligned} \tag{A4}$$

where $g_0 = m_b/2\pi\hbar^2$, $z = q/2k_F$, $u = \omega/qv_F$, m_b is the band mass, v_F is the Fermi velocity, and

$$C_\pm = \begin{cases} \frac{z\pm u}{|z\pm u|} & ,|z\pm u| > 1 \\ 0 & ,|z\pm u| < 1 \end{cases} \tag{A5}$$

$$D_\pm = \begin{cases} 0 & ,|z\pm u| > 1 \\ 1 & ,|z\pm u| < 1 \end{cases} \tag{A6}$$

In the fractional quantum Hall regime, electron-electron interactions cannot be ignored. In Chern-Simons composite fermion theory interactions enter only through the local field produced by attached flux quanta. The composite fermion polarization function is defined by

$$j^\alpha(q,\omega) = ec^2\Pi^{\alpha\beta}_{\rm CF}(q,\omega)A^\beta_{\rm CF,total}(q,\omega), \tag{A7}$$

where $\mathbf{A}_{\rm CF,total}$ is the total electromagnetic field seen by the Composite Fermions which includes the Chern-Simons field. In the RPA (MRPA) one approximates $\Pi_{\rm CF}$ by $\Pi^{(0)}$ and relates $\Pi^{\rm e}$ to $\Pi_{\rm CF}$ by[2,5]

$$[\Pi^{\rm e}]^{-1} = [\Pi_{\rm CF}]^{-1} + \mathbf{C} + \mathbf{F} \tag{A8}$$

with

$$\mathbf{C} = \frac{ec\Phi_0\tilde{\phi}}{q}\begin{bmatrix} 0 & i \\ -i & 0 \end{bmatrix} \tag{A9}$$

and

$$\mathbf{F} = \frac{\Delta m}{n_0}\begin{bmatrix} (\frac{\omega}{q})^2 & 0 \\ 0 & c^2 \end{bmatrix} \tag{A10}$$

Here $\Delta m = m^* - m_b$ where m^* it the effective mass, and n_0 is the equilibrium electron number density, $\Phi_0 = 2\pi\hbar/e$, and $\tilde{\phi} = 2$ at half filling. The difference between RPA and MRPA lies in the matrix $\mathbf{F}$ which is set to zero for the RPA. Notice that MRPA reduces to RPA if the effective mass is chosen to be equal to the band mass. Solving for $\Pi^{\rm e}_{00}$ we get (since $\Pi^{(0)}_{01} = \Pi^{(0)}_{10} = 0$)

$$\Pi^{\rm e}_{00} = \frac{\Pi^{(0)}_{00}}{1 + \frac{\Delta m}{n_0}\left(\frac{\omega}{q}\right)^2\Pi^{(0)}_{00} - \left(\frac{ec\Phi_0\tilde{\phi}}{q}\right)^2\Pi^{(0)}_{00}\Pi^{(0)}_{11}\frac{n_0}{n_0 + c^2\Delta m\Pi^{(0)}_{11}}} \tag{A11}$$

In Eq. (A11) the band mass in the expression for $\Pi^{(0)}_{00}$ is replaced by the effective mass. $\Pi^{(0)}_{11}$ is related to the current-current correlation function and is given by

$$\Pi^{(0)}_{11} = \frac{-n_0}{m^*c^2} + \frac{1}{A}\sum_{\mathbf{k}}\left(\frac{\hbar k_y}{m^*c}\right)^2\frac{n_F(\xi_{\mathbf{k}+\mathbf{q}}) - n_F(\xi_{\mathbf{k}})}{\hbar\omega - \xi_{\mathbf{k}+\mathbf{q}} + \xi_{\mathbf{k}} + i\eta} \tag{A12}$$

which at zero temperature is

$$\mathrm{Re}\Pi_{11}^{(0)} = \frac{-n_0}{m^*c^2} + (\frac{\hbar k_F}{m^*c})^2 \frac{g_0^*}{6z}\Big(3z + C_+[(z+u)^2-1]^{3/2} + C_-[(z-u)^2-1]^{3/2} - (z+u)^3 - (z-u)^3\Big) \tag{A13}$$

$$\mathrm{Im}\Pi_{11}^{(0)} = (\frac{\hbar k_F}{m^*c})^2 \frac{g_0^*}{6z}\Big(D_-[1-(z-u)^2]^{3/2} - D_+[1-(z+u)^2]^{3/2}\Big) \tag{A14}$$

with $g_0^* = m^*/2\pi\hbar^2$.

At finite temperature, the expressions for $\Pi_{00}^{(0)}$ and $\Pi_{11}^{(0)}$ must be evaluated numerically. We have done this by evaluating the angular integral analytically and expressing the functions in terms of Fermi-Dirac Integrals which are defined according to

$$\mathcal{F}_j(x,b) = \frac{1}{\Gamma(j+1)}\int_b^\infty \frac{t^j}{1+\exp(t-x)}dt. \tag{A15}$$

We find

$$(g^*)^{-1}\mathrm{Re}\Pi_{00}^{(0)} = 1 - \frac{\sqrt{\pi}\tilde{T}^{1/2}}{4z}\Big(\mathcal{F}_{-1/2}(\frac{\Omega_+^2-\tilde{\mu}}{\tilde{T}},0) - \mathcal{F}_{-1/2}(\frac{\Omega_+^2-\tilde{\mu}}{\tilde{T}},\frac{\Omega_+^2}{\tilde{T}})\Big) - \mathrm{sgn}(\Omega_-)\frac{\sqrt{\pi}\tilde{T}^{1/2}}{4z}\Big(\mathcal{F}_{-1/2}(\frac{\Omega_-^2-\tilde{\mu}}{\tilde{T}},0) - \mathcal{F}_{-1/2}(\frac{\Omega_-^2-\tilde{\mu}}{\tilde{T}},\frac{\Omega_-^2}{\tilde{T}})\Big) \tag{A16}$$

$$(g^*)^{-1}\mathrm{Im}\Pi_{00}^{(0)} = \frac{\sqrt{\pi}\tilde{T}^{1/2}}{4z}\Big(\mathcal{F}_{-1/2}(\frac{\tilde{\mu}-\Omega_-^2}{\tilde{T}},0) - \mathcal{F}_{-1/2}(\frac{\tilde{\mu}-\Omega_+^2}{\tilde{T}},0)\Big) \tag{A17}$$

$$(\frac{m^*c}{\hbar k_F})^2(g_0^*)^{-1}\mathrm{Re}\Pi_{11}^{(0)} = -u^2 - z^2/3 + \frac{\sqrt{\pi}\tilde{T}^{3/2}}{8z}\Big(\mathcal{F}_{1/2}(\frac{\Omega_+^2-\tilde{\mu}}{\tilde{T}},0) - \mathcal{F}_{1/2}(\frac{\Omega_+^2-\tilde{\mu}}{\tilde{T}},\frac{\Omega_+^2}{\tilde{T}})\Big) + \mathrm{sgn}(\Omega_-)\frac{\sqrt{\pi}\tilde{T}^{3/2}}{8z}\Big(\mathcal{F}_{1/2}(\frac{\Omega_-^2-\tilde{\mu}}{\tilde{T}},0) - \mathcal{F}_{1/2}(\frac{\Omega_-^2-\tilde{\mu}}{\tilde{T}},\frac{\Omega_-^2}{\tilde{T}})\Big) \tag{A18}$$

$$(\frac{m^*c}{\hbar k_F})^2(g_0^*)^{-1}\mathrm{Im}\Pi_{11}^{(0)} = \frac{\sqrt{\pi}\tilde{T}^{3/2}}{8z}\Big(\mathcal{F}_{1/2}(\frac{\tilde{\mu}-\Omega_-^2}{\tilde{T}},0) - \mathcal{F}_{1/2}(\frac{\tilde{\mu}-\Omega_+^2}{\tilde{T}},0)\Big) \tag{A19}$$

Here $\Omega_\pm = z \pm u$, and we have defined the dimensionless quantities $\tilde{\mu} = \mu/E_F$ and $\tilde{T} = k_BT/E_F$ where μ is the chemical potential and E_F is the Fermi energy. For parabolic bands $\tilde{\mu}/\tilde{T} = \ln(e^{1/\tilde{T}}-1)$. For evaluating the Fermi-Dirac Integrals we have used efficient algorithms that are publicly available.[49]

[1] For a review, see H. L. Stormer, in *Perspectives in Quantum Hall Effects*, Edited by S. Das Sarma and A. Pinczuk (John Wiley and Sons, Inc., New York, 1997).
[2] B. I. Halperin, P. A. Lee, and N. Read, Phys. Rev. B **47**, 7312 (1993).
[3] J. K. Jain, Phys. Rev. Lett. **63**, 199 (1989); Adv. Phys. **41**, 105 (1992)).
[4] W. Kohn, Phys. Rev. **123**, 1242 (1961).
[5] S. H. Simon and B. I. Halperin, Phys. Rev. B **48**, 17386 (1993)
[6] N. Read, Sci. Tech. **9**, 1859 (1994); Surf. Sci. **361**, 7 (1996).
[7] R. Shankar and G. Murthy, Phys. Rev. Lett. **79**, 4437 (1997).
[8] D.-H. Lee, Phys. Rev. Lett. **80**, 4547 (1998).
[9] V. Pasquier and F. D. M. Haldane, Nucl. Phys. **B 516**, 719 (1998).
[10] B. I. Halperin and A. Stern, Phys. Rev. Lett. **80**, 5457 (1998); A. Stern, B. I. Halperin, F. von Oppen, and S. Simon, Phys. Rev. B **59**, 12547 (1999).
[11] N. Read, Phys. Rev. B **58**, 16262 (1998).
[12] R. Shankar, Phys. Rev. Lett. **83**, 2382 (1999).
[13] M. P. Lilly, J. P. Eisenstein, L. N. Pfeiffer, and K. W. West, Phys. Rev. Lett. **80**, 1714 (1998).
[14] I. Ussishkin and A. Stern, Phys. Rev. B **56**, 4013 (1997).
[15] S. Sakhi, Phys. Rev. B **56**, 4098 (1997).
[16] Y. B. Kim and A. J. Millis, Physica E **4**, 171 (1999); preprint archived at cond-mat/9611125.
[17] I. Ussishkin and A. Stern, Phys. Rev. Lett. **81**, 3932 (1998).
[18] F. Zhou and Y. B. Kim, Phys. Rev. B **59** 7825 (1999).
[19] S. Zelakiewicz, H. Noh, T. J. Gramila, L. N. Pfeiffer, and K. W. West, preprint archived at cond-mat/9907396.
[20] M. C. Bønsager, K. Flensberg, B. Y.-K. Hu, and A. H. MacDonald, Phys. Rev. B **57**, 7085 (1998); Physica B **249-251**, 864 (1998).
[21] H. C. Tso, P. Vasilopoulos, and F. M. Peeters, Phys. Rev. Lett. **68**, 2516 (1992).
[22] C. Zhang and Y. Takahashi, J. Phys.: Condens. Matter **5**, 5009 (1993).
[23] S. M. Badalyan and U. Rösler, Phys. Rev. B **59**, 5643 (1999).
[24] P. M. Solomon, P. J. Price, D. J. Frank, and D. C. La Tulipe, Phys. Rev. Lett. **63**, 2508 (1989).
[25] T. J. Gramila, J. P. Eisenstein, A. H. MacDonald, L. N. Pfeiffer, and K. W. West, Phys. Rev. Lett. **66**, 1216 (1991); Surf. Sci. **263**, 446 (1992).
[26] T. J. Gramila, J. P. Eisenstein, A. H. MacDonald, L. N. Pfeiffer, and K. W. West, Phys. Rev. B **47**, 12957 (1993);

Physica B **197**, 442 (1994).
[27] U. Sivan, P. M. Solomon, and H. Shtrikman, Phys. Rev. Lett. **68**, 1196 (1992).
[28] C. Jörger, S. J. Cheng, H. Rubel, W. Dietsche, R. Gerhardts, P. Specht, K. Eberl, and K. v. Klitzing, preprint archived at cond-mat/9904214.
[29] A.-P. Jauho and H. Smith, Phys. Rev. B **47**, 4420 (1993).
[30] L. Zheng and A. H. MacDonald, Phys. Rev. B **48**, 8203 (1993).
[31] A. Kamenev and Y. Oreg, Phys. Rev. B **52**, 7516 (1995).
[32] K. Flensberg, B. Y.-K. Hu, A.-P. Jauho, and J. Kinaret, Phys. Rev. B **52**, 14761 (1995).
[33] B. Y.-K. Hu, Phys. Rev. B **57**, 12345 (1998).
[34] K. Güven and B. Tanatar, Solid State Comm. **104**, 439 (1997); Phys. Rev. B **56**, 7535 (1997);
[35] P. J. Price, Ann. Phys. (N.Y.) **133**, 217 (1981).
[36] S. K. Lyo, Phys. Rev. B **38**, 6345 (1988).
[37] A. G. Rojo, J. Phys.: Cond. Mat. **11**, R31 (1999).
[38] K. Flensberg and B. Y.-K. Hu, Phys. Rev. Lett. **73**, 3572 (1994); Phys. Rev. B **52**, 14796 (1995).
[39] N. P. R. Hill *et al.*, Phys. Rev. Lett. **78**, 2204 (1997).
[40] N. Noh, S. Zelakiewicz, X.-G. Feng, T. J. Gramila, L. N. Pfeiffer, and K. W. West, Phys. Rev. B **58**, 12621 (1998).
[41] D. V. Khveshchenko, preprint archived at cond-mat/9812093.
[42] N. Noh, S. Zelakiewicz, T. J. Gramila, L. N. Pfeiffer, and K. W. West, Phys. Rev. B **59**, 13114 (1999).
[43] S. Melinte et al., Phys. Rev. Lett. **84**, 354 (2000).
[44] A. E. Dementyev et al., Phys. Rev. Lett. **83**, 5074 (1999).
[45] Y. B. Kim, A. Furusaki, X.-G. Wen, and P. A. Lee, Phys. Rev. B **50**, 17917 (1994).
[46] B. L. Altshuler, L. B. Ioffe, and A. J. Millis, Phys. Rev. B **50**, 14048 (1994).
[47] M. C. Bønsager, Y. B. Kim, and A. H. MacDonald, work in progress.
[48] F. Stern, Phys. Rev. Lett. **18**, 546 (1967).
[49] We have used a FORTRAN code authored by Allan MacLeod and Michele Goano available from http://www.netlib.org See also, M. Goano, Solid-State Electronics, **36**, 217 (1993).

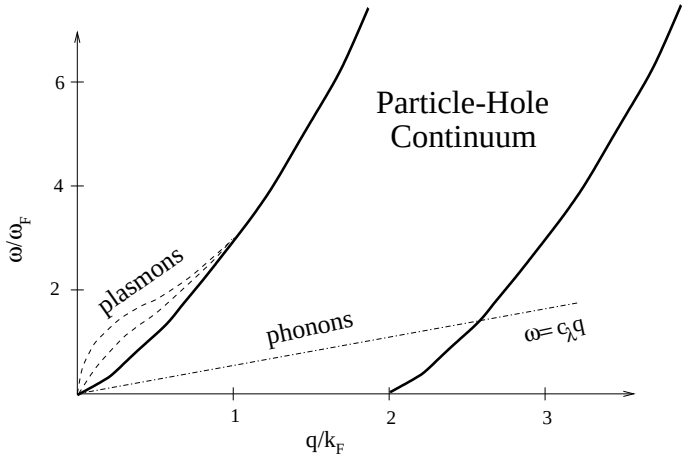

FIG. 1. A sketch of the (q,ω)-space on which the integrand of Eq. (2) is defined. At zero temperature $\mathrm{Im}\Pi(q,\omega)$ is zero outside the particle-hole continuum. However, at finite temperature the integrand will have finite weight at the position of the plasmon poles indicated by the dashed lines.[38] (There are two plasmon poles whose exact position and strength depend on the interlayer distance). The dash-dotted line shows the phonon resonance. Phonon mediated drag is dominated by contributions from this resonance for as high as possible q limited by $\omega < T$.

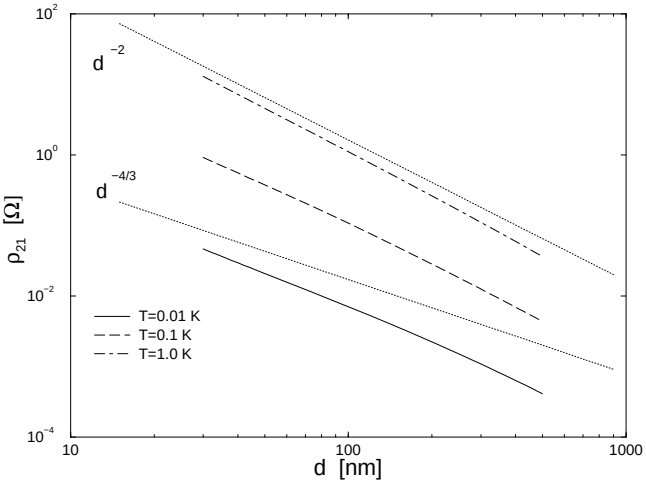

FIG. 2. The Coulomb contribution to the transresistivity calculated as a function of distance between the layers using the RPA with $m^* = m_e$. The two dotted lines indicate the power laws $d^{-4/3}$ and d^{-2}, respectively. The calculations are based on Eq. (2) and the RPA for composite fermions.

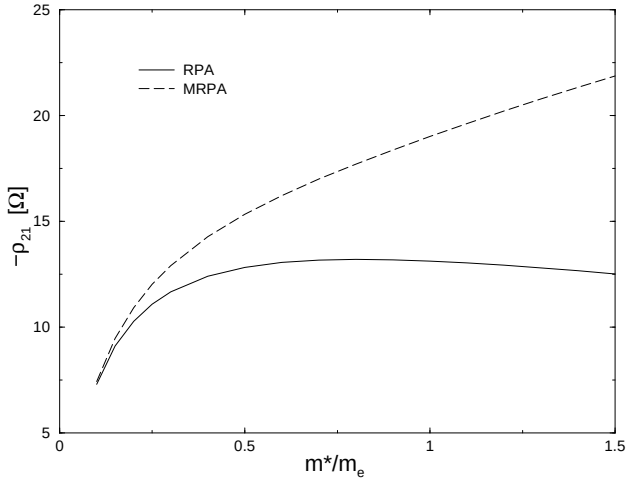

FIG. 3. The dependence on effective mass of the Coulomb contribution to the transresistivity. The temperature is 1 K (notice that there is no mass dependence for $T \to 0$). Other parameters are $d = 300$ Å, $L = 200$ Å, and $n = 1.5\times10^{15}$ m^{-2}.

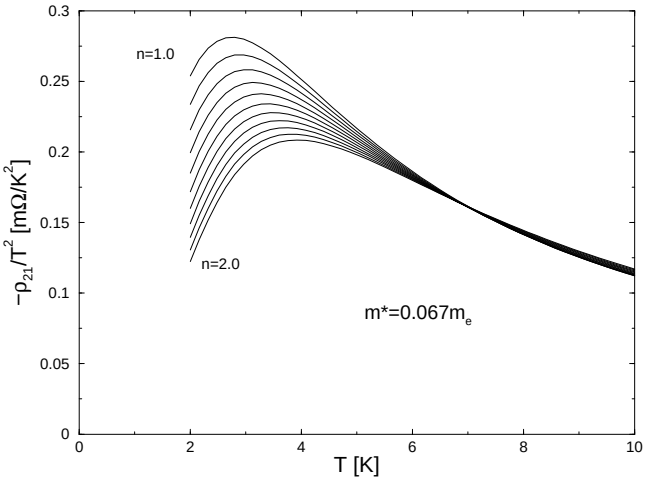

FIG. 4. Scaled transresistivity as a function of temperature for $m^* = m_b = 0.067m_e$. The 11 curves are calculations for the density ranging from $n = 1.0 \times 10^{15}$ m^{-2} to $n = 2.0 \times 10^{15}$ m^{-2} in increments of $n = 0.1 \times 10^{15}$ m^{-2}. Other parameters are $d = 5000$ Å, $L = 200$ Å, and $\ell_{\rm ph} = 100$ μm. For $n = 1.5 \times 10^{15}$ m^{-2} the Fermi temperature is 62.3 K. These calculations are based on the MRPA; corresponding calculations based on the RPA show almost identical results.

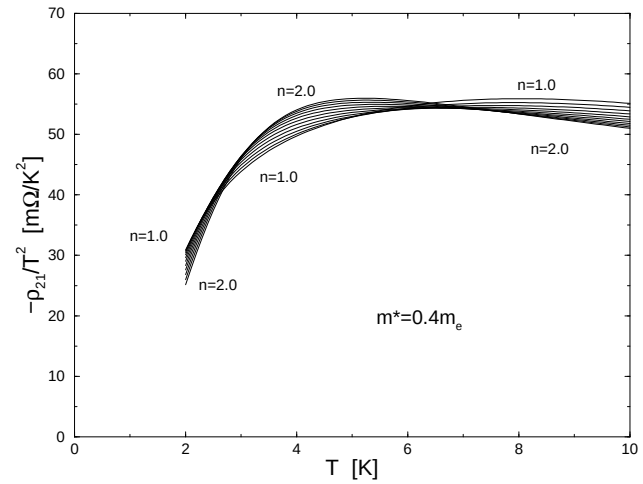

FIG. 5. The same as in Fig. 4 but with $m^* = 0.4m_e$. For $n = 1.5 \times 10^{15}$ m^{-2} the Fermi temperature is 10.4 K.

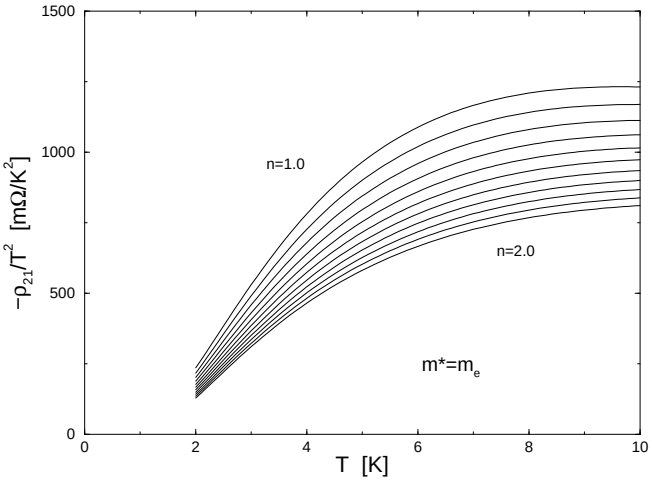

FIG. 6. The same as in Fig. 4 but with $m^* = m_e$. For $n = 1.5 \times 10^{15}$ m^{-2} the Fermi temperature is 4.2 K.

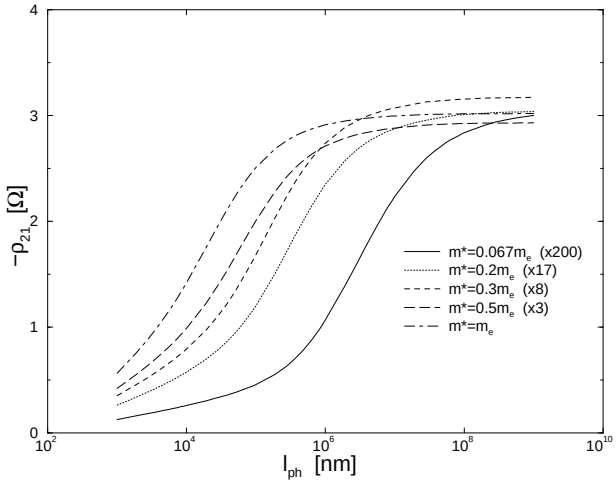

FIG. 7. The transresistivity as a function of phonon mean free path for different values of the effective mass. The plot shows how the critical phonon mean free path $\ell_{\rm crit}$ decreases with increasing m^*. Here, the temperature is 3 K and the distance is $d = 500$ Å.